Realization of a martensitic phase transition in $KFeF_4$ under high pressure

1995 J. Phys.: Condens. Matter 7 825

(http://iopscience.iop.org/0953-8984/7/5/004)

J. Phys.: Condens. Matter 7 (1995) 825–835. Printed in the UK

Realization of a martensitic phase transition in $KFeF_4$ under high pressure

Q Wang†, A Bulou, A Désert and J Nouet

Laboratoire de Physique de l'Etat Condensé (Unité associée au CNRS 807), Université du Maine, 72017 Le Mans Cedex, France

Received 31 May 1994, in final form 24 October 1994

Abstract. The room-temperature Raman spectra of $KFeF_4$ (phase II) were measured under high pressures up to 3.5 GPa. The pressure dependence of the frequencies exhibits strong changes at 1.2 GPa and minor changes at 2.2 GPa. The former is attributed to a martensitic phase transition leading to the so-called $TlAlF_4$-type structure. A hysteresis of about 0.15 GPa is observed. A strong hardening of two modes under pressure suggests that the phase change is achieved because of octahedra rotations which weaken the clamping between successive octahedra sheets. The singularity at 2.2 GPa presumably arises from a quasi-reversible phase transition in the $TlAlF_4$-type structural arrangement. The vibrational frequencies are discussed in comparison with those obtained in isomorphous compounds.

1. Introduction

The AMF_4 compounds ($A \equiv K^+, Rb^+, Tl^+, \ldots$; $M \equiv Al^{3+}, Fe^{3+}, Ti^{3+}, \ldots$) undergo a wide variety of structural phase transitions (SPTs). They are built of MF_6 octahedra sheets and they mainly belong to two‡ different structural arrangements. One is the $TlAlF_4$-type structure [1–6] (denoted hereafter TAt) shown in figure 1(a) which consists of infinite superimposed AlF_6 octahedra sheets; in the higher-symmetry (prototypic) phase (called phase I), which is tetragonal and observed for example in $RbAlF_4$ and in $RbFeF_4$ at high temperatures, each MF_6 octahedron is centred in a square-based parallelepiped of cation A^+ (figure 1(b)). In such a structural arrangement, several quasi-reversible SPTs associated with octahedra rotations are observed on cooling [2–5]. $KAlF_4$ crystallizes with this arrangement at high temperatures with an octahedra rotation around the [001] axis (this phase is usually denoted phase II).

The second important structural arrangement (figure 2) is the so-called $KFeF_4$-type structure [9–13] (denoted KFt), also observed in $KAlF_4$ at low temperatures [3] (phase IV). The ideal structure from which they derive is presented in figure 2(b). In fact, such an idealized structure is not observed since the corresponding space group allows octahedra rotations around the [100] axis and K^+ displacements along the [001] axis as schematized by the arrows in figure 2(b). SPTs associated with octahedra rotations around the [010] and [001] axes are also observed [3, 9–13].

A transition between these two structures was encountered in $KAlF_4$ at about 260 K (ambient pressure) from phase II (TAt structure) to phase IV (KFt structure) [3], or at 0.21 GPa (300 K) from phase IV to phase II [14]. This phase transition presents the main

† Permanent address: Physics Department, Harbin Normal University, 150080 Harbin, People's Republic of China.

‡ Different structures such as β-$RbAlF_4$ [7] and $KCrF_4$ [8] are also known.

0953-8984/95/050825+11$19.50

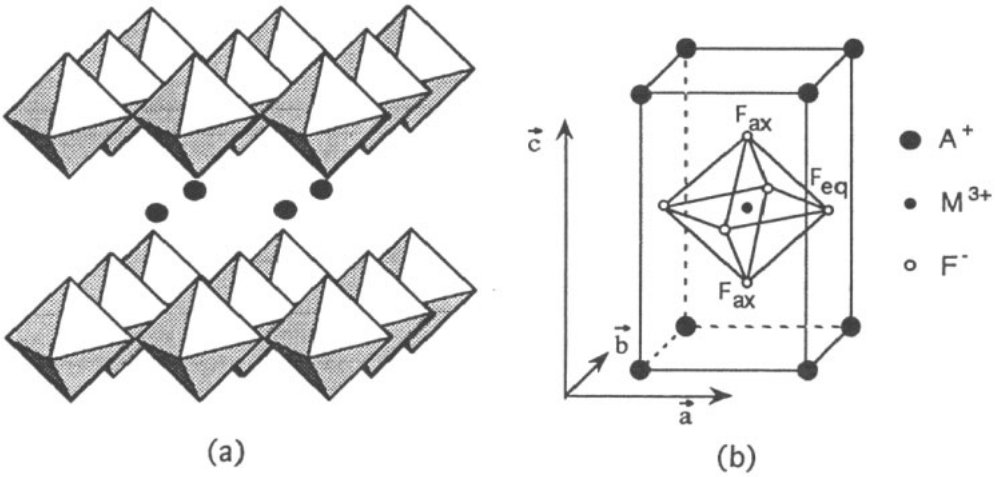

Figure 1. (a) AlF_6 octahedra sheets of the $TlAlF_4$-type structure and (b) the unit cell of the ideal phase.

characteristics of the so-called martensitic phase transitions (MPTs), including the existence of a pre-martensitic phase [15].

$KFeF_4$ has the same type of structure as $KAlF_4$ in phase IV and it undergoes a SPT at about 390 K (ambient pressure) between phase I (KFt phase; space group, $Bmmb(D_{2h}^{17})$; $Z = 4$) and phase II (KFt phase; space group, $Pcmn(D_{2h}^{16})$; $Z = 8$) mainly associated with octahedra rotations around the [001] and [010] axes (figure 3). Until now no MPT has been reported in this compound. However, two A_g symmetry modes (at 152 and 98 cm^{-1} at room temperature) have been shown to exhibit a soft character on heating [13]. They correspond to librations of the octahedra around the [100] axis with K^+ vibrations along [001] which is equivalent to the X_3^1 mode in $KAlF_4$ (phase II); this mode softens when the MPT temperature is approached from above [16]. So, it is reasonable to think that a MPT could occur in $KFeF_4$. According to [3], the molecular volume of $KAlF_4$ in its TAt phase is smaller than the molecule volume in its KFt phase. So, from this consideration too, it can be predicted that, under high pressures, a compound belonging to the latter type should evolve towards the former type. This work is aimed at realizing a MPT in $KFeF_4$ under high pressures. The Raman scattering investigation was employed to detect the phase transition since, as shown in [14], such a phase change strongly affects the vibrational spectra.

2. Experiment

The hydrostatic pressures, up to 3.5 GPa, were generated by a gasketed diamond anvil cell of Merrill–Bassett [17] type in combination with the ruby luminescence method for pressure determination [18] (the R_1 and R_2 lines of ruby shift linearly with pressure to lower frequencies according to the relation P (GPa) $= 0.133|\Delta\nu|$ (cm^{-1}) which is valid up to 20 GPa). A 4:1 methanol:ethanol mixture was used as the pressure medium which can ensure a truly hydrostatic pressure up to 10 GPa or more [19]. The experiments have been performed under a microscope (micro-Raman system) with a DILOR-Z24 triple monochromator instrument. The Raman signal was excited by the 514.5 nm line of an argon ion laser (Coherent 90-3) and the typical power was 7 mW just before introduction

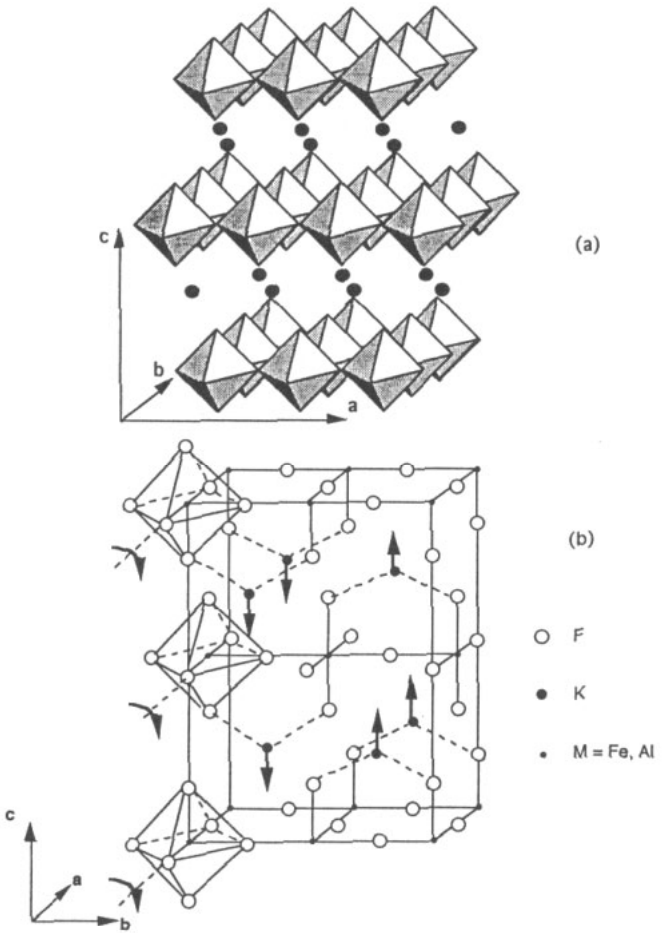

Figure 2. (a) FeF_6 octahedra sheets of the $KFeF_4$-type structure and (b) the unit cell of the ideal phase. The arrows represent the rotations and displacements by the symmetry of the ideal phase.

in the cell. Under the experimental conditions, the typical resolution was 7 cm^{-1} (with a slit width of 700 μm). The cylindrical pressure chamber of about 100 μm height and 200 μm diameter was drilled in an Inconel stainless-steel gasket. The sample consists of several crystal sheets about 150 μm wide and 20 μm thick. The crystal sheets were placed in the pressure chamber one on top of the other and mainly oriented with the c axis (normal to the sheets) parallel to the laser beam (but without mutual orientation of the a and b crystallographic axes) and so the diffusion geometries investigated were mainly $Z(XX)Z$, $Z(YY)Z$ and $Z(XY)Z$.

3. Results

From macro-Raman studies on $KFeF_4$ single crystals, Désert *et al* [13] reported 19 Raman lines at room temperature (and ambient pressure) while in the diamond anvil cell, where

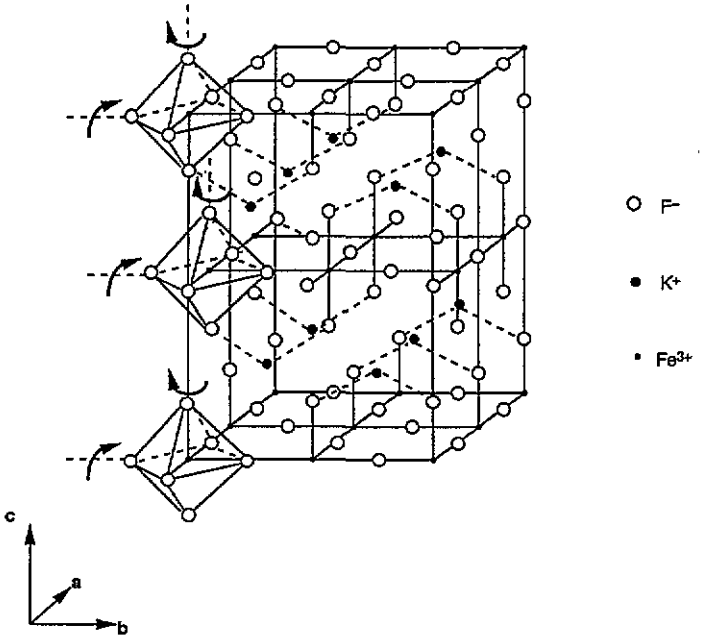

Figure 3. Ionic arrangements in $KFeF_4$ phase II (room temperature and ambient pressure). Only the additional rotations that occur in phase II are represented (by curved arrows).

the diffusion geometry is mainly $Z(XX)Z$, $Z(YY)Z$ and $Z(XY)Z$, only 11 lines can be unambiguously observed with significant intensity (figure 4). Their labelling, intensities and frequencies (at room temperature and ambient pressure) are given in table 1. The frequencies are in good agreement with those reported by Désert *et al* [13] except for the weak l_8 signal not mentioned in this article. All these lines undergo continuous frequency variations up to 1.2 GPa (figures 4 and 5). At this pressure, most of them vanish and a strong 'background' appears in the whole spectrum (figure 4). Only the line l_1 (at 521 cm^{-1}) plus a new line at 542 cm^{-1} (l'_1) are observed. On increasing the pressure again, l_1 vanishes and l'_1 increases markedly. New lines appear also at 409 cm^{-1} (l'_2), 309 cm^{-1} (l'_3), 193 cm^{-1} (l'_5), 176 cm^{-1} (l'_6), 151 cm^{-1} (l'_7), 125 cm^{-1} (l'_8), 110 cm^{-1} (l'_9), 86 cm^{-1} (l'_{10}) and 42 cm^{-1} (l'_{11}). On increasing the pressure, the signal in the vicinity of 309 cm^{-1} (l_3) appears to 'split' into l'_3 and l''_3 (307 cm^{-1} and 312 cm^{-1}, respectively, at 1.5 GPa). l'_3, l''_3, l'_5 and l'_7 become strong and l'_1 becomes very strong. It can also be noted that the l'_{11} frequency (located at 60 cm^{-1} at 1.73 GPa) is strongly pressure dependent, i.e. it could be the soft mode of some phase transition.

The pressure dependences of the frequencies of these lines are given in figure 5. In addition to the strong discontinuity at 1.2 GPa, several anomalies occur at 2.2 GPa; some lines vanish and the frequency of l'_2, which decreases with increasing pressure between 1.2 and 2.2 GPa, increases rapidly subsequently.

4. Discussion

From the above results, it appears that $KFeF_4$ undergoes a discontinuous (first-order) phase transition at 1.2 GPa. The most important effect is the strong shift in the frequency of the

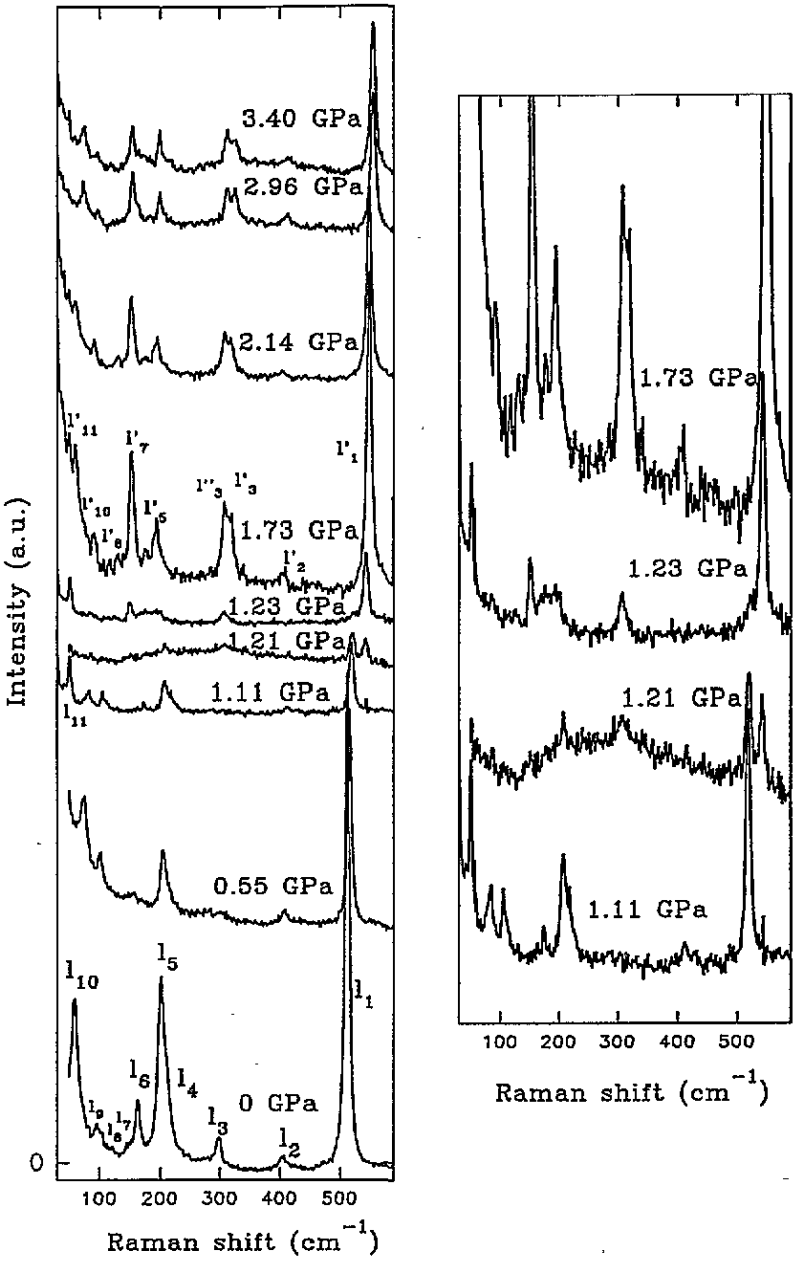

Figure 4. Pressure dependence of the Raman spectrum of $KFeF_4$ at room temperature (a.u., arbitrary units).

line l_1–l'_1. The corresponding mode, characteristic of these layer materials, is associated with vibrations of the axial fluorine ions normally to the $M^{III}F_6$ octahedra sheets (figure 6). The large discontinuity in its frequency results from a drastic change in the surrounding of the F_{ax} ions along the [001] direction and this was observed only at the MPT of $KAlF_4$ [14] where it jumped from 543 cm^{-1} in the TAt structure to 532 cm^{-1} in the KFt structure. So

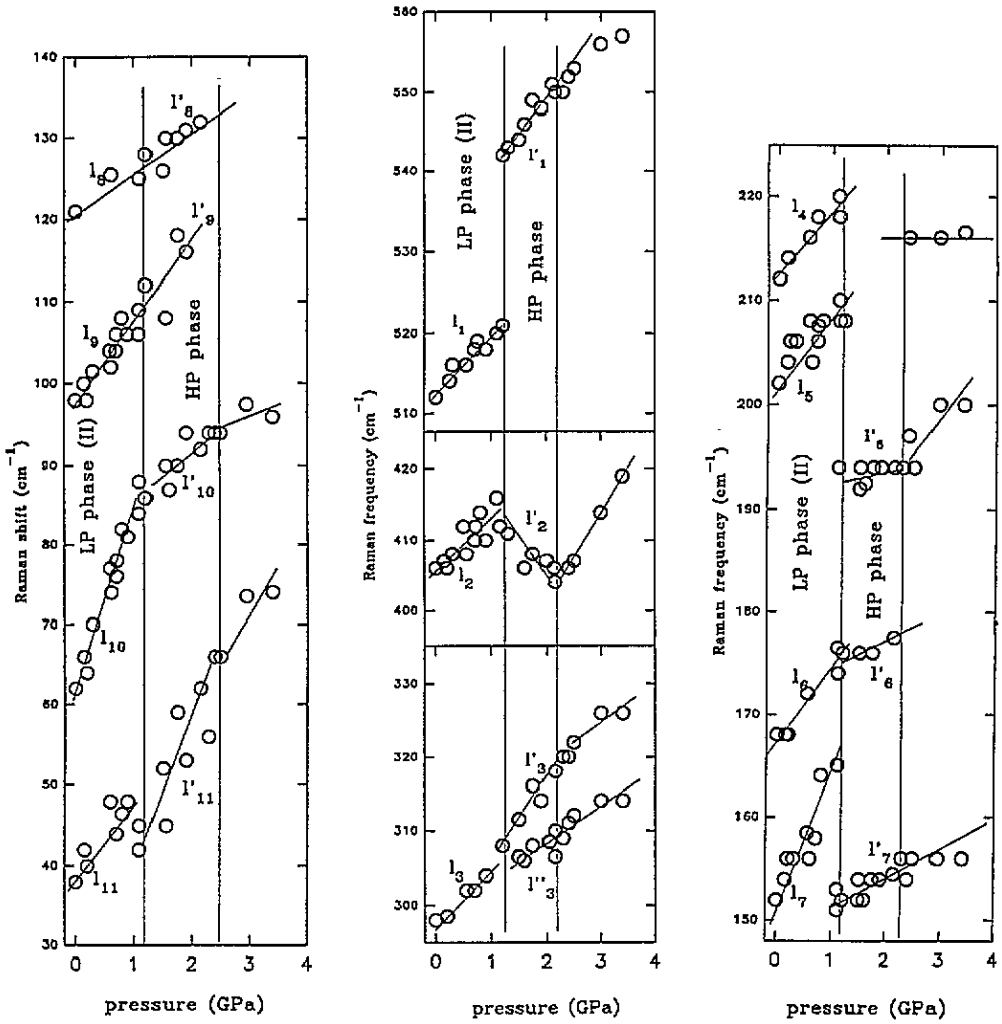

Figure 5. Pressure dependence (LP, low pressure; HP, high pressure) of the Raman frequency $\omega(P)$ of $KFeF_4$ at room temperature: ——, guides for the eye.

it can be postulated that the phenomenon observed at 1.2 GPa in $KFeF_4$ also results from a MPT; while the low-pressure phase belongs to the so-called KFt structure, the high-pressure phase belongs to the TAt structure.

4.1. Pressure dependence of the frequencies in the low-pressure phase

As the space group of phase II of $KFeF_4$ is $Pcmn(D_{2h}^{16})$ with eight formula units and 48 atoms per cell, 72 Raman-active modes are predicted (20 Ag, 16 B_{1g}, 20 B_{2g} and 16 B_{3g}); in [13], Désert *et al* give an assignment for the 19 lines experimentally observed. This will be used to attribute the 11 lines observed in the diamond anvil cell and to describe the normal coordinates of vibration associated with most of them (figure 6). The mode Grüneisen parameters [20] are given in table 1.

As already mentioned, the line l_1 (L_4 in [13]), with Ag symmetry, corresponds to the symmetric stretching of the Fe–F_{ax} bond. According to the spectra given in [13], the line

Table 1. Labelling l_i, intensity I_i, room-temperature and ambient-pressure frequency ω_i and mode Grüneisen parametres γ_i for the Raman lines of $KFeF_4$ in the low-pressure phase. The mode Grüneisen parameters are multiplied by $10^3\beta$ where β represents the (unknown) isothermal compressibility coefficient [20].

l_i	Symmetry	I_i	ω_i (cm^{-1})	$10^3\gamma_i\beta$ (GPa^{-1})
l_1	A_g	Very strong	512	15
l_2	B_{1g}	Weak	406	21
l_3	A_g	Medium	298	22
l_4	B_{2g}	Strong	212	24
l_5	B_{1g}, B_{3g}	Strong	202	29
l_6	B_{3g}	Medium	168	40
l_7	A_g	Weak	152	71
l_8		Very weak	121	34
l_9	A_g, B_{2g}	Weak	98	119
l_{10}	A_g	Strong	62	349
l_{11}		Weak	38	219

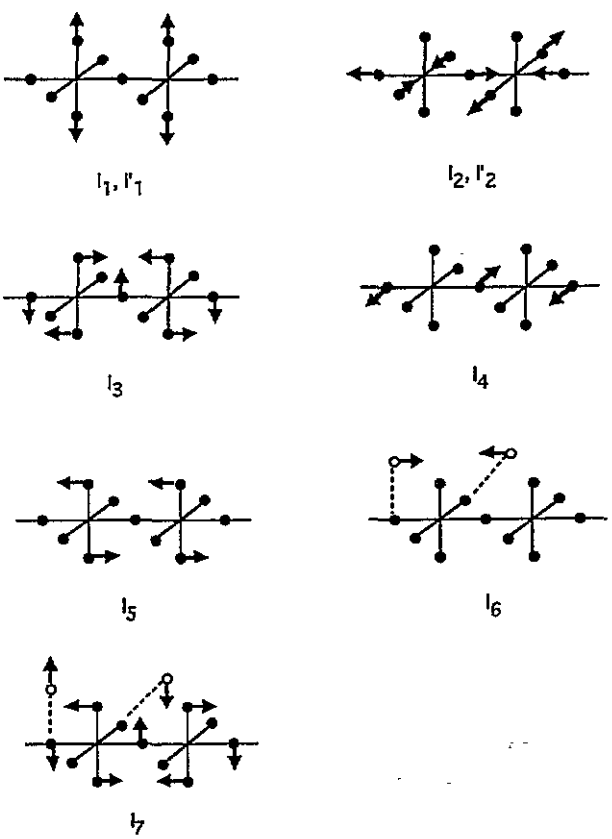

Figure 6. Schematization of the normal coordinates of vibration of $KFeF_4$ for Raman active modes in the low-pressure phase (l_i) and in the high-pressure phase (l'_i): ●, fluorine ions; ○, potassium ions.

l_2 (L_6 in [13]) is Raman inactive in phase I (as can be seen in figure 6, it is a zone boundary mode of the phase I Brillouin zone) and its intensity increases considerably in phase II. The symmetry is B_{1g}, i.e. it can be seen in the XY geometry which was a highly favourable configuration in the present experiments. The line l_3 is the A_g symmetry line L_7 of [13], active in phase I (the B_{2g} line that exists in phase II in the same frequency range probably does not give a significant contribution owing to its weak intensity [13]). The line l_4 corresponds to the strong line L_{10} of [13] with B_{2g} symmetry (ZX geometry). The line l_5 (L_{11} in [13]), which overlaps l_4, is presumably composed of two lines, one with B_{1g} symmetry and one with B_{3g} symmetry (YZ geometry), which (partly) explains the apparent dispersion of the data points in figure 5. All the above vibrations are related to octahedra distortions (figure 6). On the other hand, the line l_6 (L_{13} in [13]), with B_{3g} symmetry, is attributed to vibrations of the potassium ions (along [010]). The weak l_7 signal is an A_g symmetry line (L_{14} in [13]). Its frequency exhibits a strong temperature dependence and it is also significantly more sensitive to pressure than are the other modes in the same frequency range (table 1). It corresponds to octahedra librations around the [100] axis and to potassium vibrations along the [001] axis. The weak line l_8 cannot be identified since it is not reported in [13]. The line l_9 probably results from the overlap of two lines with A_g and B_{2g} symmetries; the former corresponds to octahedra librations around [100] with potassium vibrations along [001] and the latter is associated with potassium vibrations alone along [100]. The frequency of the Ag mode is sensitive to temperature and its pressure dependence is significant too. The line l_{10} (L_{19} in [13]) is the Ag symmetry soft mode associated with the phase I–phase II transition (Raman inactive in phase I). It is also strongly pressure dependent. The last line (l_{11}) is presumably the line L_{20} of [13].

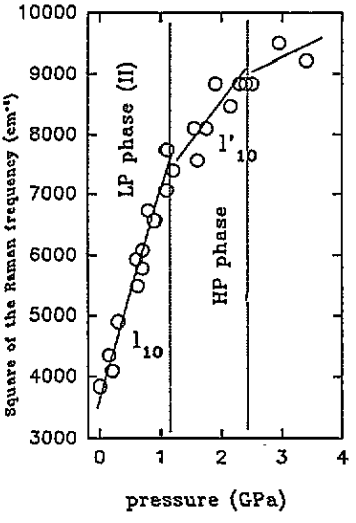

Figure 7. Pressure dependence (LP, low pressure; HP, high pressure) of the square of the frequency of the Raman line, l_{10}: ——, guides for the eye.

In [13], it was postulated that the displacive (non-martensitic) phase I–phase II transition (resulting from FeF_6 octahedra rotations around the [001] axis) is associated with the softening of a quasi-flat phonon branch which has been recently confirmed by inelastic neutron scattering experiments [21]. In this case, as was done for $RbAlF_4$, in spite of the

first-order character, the transition can be described by the Landau theory for second-order phase transitions. Hence, it is predicted that [14], at a given temperature, the square of the frequency of the soft mode (line l_{10}) should evolve linearly with pressure:

$$\omega^2 \propto P - P_c$$

where P_c represents the pressure at which the phase transition would take place if the soft phonon did not belong to a flat branch (a demonstration is given in [14] for the slightly different system $RbAlF_4$). As shown in figure 7, the experimental results are not inconsistent with such a law. In the framework of this model, one obtains $P_c = -1.2$ GPa and so it can be predicted [14] that the octahedra tilt angle around the [001] axis, which is 7.3° at room temperature and ambient pressure [11, 12], becomes 11° at 1.2 GPa where the MPT occurs. A direct measurement of the pressure dependence of this angle (by diffraction) could be used to check the validity of the model.

Concerning the mechanism inducing the MPT, it was postulated in [13] that it could be associated with a softening of the modes labelled l_7 and l_9 since the corresponding normal coordinates are strongly connected with the ionic displacements involved in the shear process. In fact, both of them harden under pressure. This is presumably associated with the increase in the tilt angle around the [100] axis, as usually observed below phase transitions owing to octahedra rotations [22]. As a consequence, the clamping between the octahedra sheets becomes weaker according to the process proposed by Bulou *et al* [16] which makes it possible that the glidings lead to the high-pressure phase. While in [16], owing to the symmetry, a dynamical libration was necessary to explain the weakening of the clamping, in the present case this can be achieved by a static rotation. To check this mechanism, it would be useful to measure the octahedra tilt angle around the [100] axis on approaching the MPT. This could be more easily performed by a powder diffraction study as a function of temperature in the low-temperature phase of the quasi-isomorphous $KAlF_4$.

As mentioned in section 3, in a narrow pressure range around the MPT, most of the Raman lines disappear while strong scattering increases in almost the whole frequency range investigated (figure 4). Such an uncommon phenomenon can be attributed to the vanishing of the long-range ordering, i.e. a 'quasi-amorphous state'. With regard to the structural rearrangement required at the MPT, it can be thought that in this intermediate 'state' the FeF_6 octahedra sheets (which are presumably preserved but possibly crinkled) are strongly disordered with respect to one another. In other words, the apparent coherent shear associated with the MPT would be a consequence of an incoherent shear of the octahedra sheets (activated by octahedra rotations, as explained above) followed by an ordering process. The scattered signal in the intermediate 'state' would be the signature of the density of states, as in an amorphous material. To explain the mechanism of the MPT, it would be useful to check for the existence of a similar behaviour in the case of $KAlF_4$, as a function of pressure and as a function of temperature (note, however, that some structural characteristics of the KFt phase of $KAlF_4$ indicate that the MPT could result from a coherent shear [3]).

4.2. Pressure dependence of the frequencies in the high-pressure phase

With regard to the behaviour of the line l_1–l_1', it can be thought that the high-pressure phase belongs to the TAt structure, like $RbFeF_4$ [5]. In the archetypal tetragonal phase (D^1_{4h} space group), two modes are Raman active (with a strong intensity), one with A_{1g} symmetry associated with the stretching of the M^{III}–F_{ax} bond and one with E_g symmetry where the F_{ax} vibrate symmetrically, parallel to the sheets (and observed in the XZ and YZ

geometries). In $RbFeF_4$, at room temperature, they are located at 531 cm^{-1} and 184 cm^{-1}, respectively [5]; in the case of the high-pressure $KFeF_4$ phase, they correspond to the lines l'_1 and l'_5, respectively (the latter having a fairly weak intensity owing to an unfavourable geometry of analysis). The slightly higher frequencies are attributed to the fact that the interionic distances are smaller since the ionic radius of potassium is smaller than that of rubidium [23]. In fact, the real symmetry is smaller than the archetype since several additional Raman lines are observed. This is usually the consequence of phase transitions by octahedra rotations; for example, the sequence of transitions encountered as a function of temperature in $RbFeF_4$ [24] is, using an extended Glazer [25] notation [2]:

$$\begin{array}{ccccccc} a_p^+b_p^-c^0 & \rightarrow & a_p^+b_p^+c^+ & \rightarrow & a^0b^0c^+ & \rightarrow & a^0b^0c^0. \\ \text{(phase IV)} & & \text{(phase III)} & & \text{(phase II)} & & \text{(phase I)} \\ (Pmab) & & (Pmmn) & & (P\tfrac{4}{m}bm) & & (P\tfrac{4}{m}mm). \end{array}$$

The number of lines is even greater than the number expected in phase II; in fact, the Raman spectra in the high-pressure phase of $KFeF_4$ look very much like those of $RbFeF_4$ in phase IV [5]. In this framework, the line l'_2 would correspond to the same mode as the line l_2 (L3 in [5]); l'_3 and l'_4 would correspond to the L4 and L5 in [5] attributed to the M_7, M_9^1 and X_3^3 (as for l_3) modes of the archetype. As discussed above, l'_5 arises from the $\Gamma_9(E_g)$ mode of the archetype; in fact, owing to its degeneracy, a splitting is expected in the orthorhombic phase IV, which could explain the shoulder of this line on the high-frequency side (figure 4). The strong line l'_7 at 152 cm^{-1} probably corresponds to the L11 line of $RbFeF_4$ (observed in the XY geometry) at 105 cm^{-1} at room temperature. It arises from the X_1 mode involving cation displacements and the value obtained in $KFeF_4$ is in good agreement with the value (155 cm^{-1}) predicted from the frequency in $RbFeF_4$ and the potassium-to-rubidium mass ratio (assuming similar force constants). The low-frequency mode exhibits a soft character and is presumably associated with a (virtual) phase transition to a higher-symmetry phase. The square of its frequency follows a linear behaviour and, in the absence of the MPT, this phase transition should occur at 0.15 GPa.

In the absence of polarization analysis, attributing the other low-frequency and low-intensity lines is more difficult since many modes may exist in this frequency range.

In this high-pressure phase, a weak singularity is also observed in the vicinity of 2.2 GPa (some lines vanish while new lines appear, and slope changes are observed). However, since the structure of the high-pressure phase remains questionable, it is difficult to predict the origin of the phenomenon. It can be thought that it should occur also in the (presumably) isostructural $RbFeF_4$ where the structure is well established. So, this would be a better system for the investigation of what seems to be a new behaviour.

5. Conclusion

In this work it has been shown for the first time, by Raman scattering, that $KFeF_4$ undergoes a MPT at 1.2 GPa; the structure changes from the so-called $KFeF_4$-type structure at low pressures to the $TlAlF_4$-type structure at high pressures. It is established that the two modes that were thought to be associated with such a phase transition are strongly pressure dependent. It is deduced that the MPT is presumably induced by an increase in the (static) octahedra rotation angles around the [100] axis while the reverse transition (as observed in $KAlF_4$) was associated with the softening of (dynamical) octahedra librations around the same axis. To check this mechanism, it would be useful to perform measurements of

this rotation angle on approaching the MPT in the $KFeF_4$-type structure. The isomorphous $KAlF_4$, which undergoes a MPT as a function of pressure and temperature as well, would probably be a better system to perform such an investigation. It must also be pointed out that most of the Raman lines disappear at the MPT while a strong 'background' appears, which could be explained by (partial) amorphization of the compound. This should be checked too.

According to the Raman spectrum, it can be thought that the high-pressure phase has the same structure as $RbFeF_4$ at room temperature (space group, *Pmab*). An additional phase transition has been observed in this high-pressure phase but its exact origin remains to be explained. This could probably be achieved by a pressure study of $RbFeF_4$.

Acknowledgments

The authors wish to thank G Niesseron for growing the samples and Professor M Rousseau for fruitful comments.

References

[1] Brosset C 1937 *Z. Anorg. (Allg.) Chem.* **235** 139
[2] Bulou A and Nouet J 1982 *J. Phys. C: Solid State Phys.* **15** 183
[3] Launay J M, Bulou A, Hewat A W, Gibaud A, Laval J Y and Nouet J 1985 *J. Physique* **46** 771
[4] Bulou A and Nouet J 1987 *J. Phys. C: Solid State Phys.* **20** 2885
[5] Pique C, Bulou A, Moron M C, Burriel R, Fourquet J L and Rousseau M 1990 *J. Phys.: Condens. Matter* **2** 8277
[6] Bulou A, Rousseau M, Nouet J and Hennion B 1989 *J. Phys.: Condens. Matter* **1** 4553–83
[7] Fourquet J L, Plet F and De Pape R 1980 *Acta Crystallogr.* B **36** 1997–2000
[8] Dewan J C and Edwards A J 1977 *J. Chem. Soc., Chem. Commun.* 533–4
[9] Heger G, Geller R and Babel D 1971 *Solid State Commun.* **9** 335
[10] Hidaka M, Garrard B J and Wanklyn B M R 1984 *Phys. Rev.* B **30** 3649
[11] Sciau P and Grébille D 1989 *Phys. Rev.* B **39** 11 982
[12] Désert A 1990 *PhD Thesis* Université du Maine
[13] Désert A, Bulou A and Nouet J 1992 *J. Phys.: Condens. Matter* **4** 1023
[14] Wang Q, Ripault G and Bulou A 1994 *Phase Transitions* at press
[15] Gibaud A, Bulou A, Le Bail A, Nouet J and Zeyen C M 1987 *J. Physique* **48** 1521–32
[16] Bulou A, Gibaud A, Debieche M, Nouet J, Hennion B and Petitgrand D 1989 *Phase Transitions* **14** 47
[17] Merrill L and Bassett W A 1974 *Rev. Sci. Instrum.* **45** 290
[18] Mao H K and Bell P M 1978 *Science* **200** 1145
[19] Piermarini G J, Block S and Barnett J D 1973 *J. Appl. Phys.* **44** 5377
[20] Jayaraman A 1983 *Rev. Mod. Phys.* **55** 65
[21] Désert A 1994 to be published
[22] Boulesteix C 1992 *Diffusionless Phase Transitions and Related Structures in Oxides* (Aedersmannsdorf: Trans Tech)
[23] Shannon R D 1976 *Acta Crystallogr.* A **32** 751
[24] Moron M C, Bulou A, Pique C and Fourquet J L 1990 *J. Phys.: Condens. Matter* **2** 8269–75
[25] Glazer A M 1975 *Acta Crystallogr.* A **31** 756